

CORRECTION

Correction: Reducing gravity takes the bounce out of running
(doi:10.1242/jeb.162024)

Delyle T. Polet, Ryan T. Schroeder and John E. A. Bertram

There were two errors published in *J. Exp. Biol.* (2018) **221**, jeb162024 (doi:10.1242/jeb.162024).

First, a single coefficient A was used to denote what should have been three separate proportionality constants. Three distinct uses of A were:

A_1 : $E_{\text{freq}}=A(g/V)^k$, used in Eqn 1, with units of J s^k ,

A_2 : $E_{\text{freq}}=A_f^k$, used in the list of symbols and in the caption to Fig. 4, also with units of J s^k ,

A_3 : $V=A\sqrt{g}$, used in Appendix 2, and in Eqns 3 and A15, with units of $\sqrt{\text{m}}$.

For impulsive running, $A_2=2^k A_1$. By setting $k=2$, taking the derivative of Eqn 1 with respect to V and setting to zero, we can solve for A_3 in terms of A_1 , and find $A_3=(2A_1/m)^{1/4}$, for A_1 at $k=2$.

Second, a missing exponent in the code generating Fig. 4 led to improperly scaled axes. Although each axis should be down-scaled, the relative shape of the curves is unchanged in the corrected figure (see below). The optimal take-off velocities in the corrected figure correspond approximately to those of the best fit in Fig. 2B for each level of gravity.

The premise and conclusions of the paper are unchanged. The authors would like to thank the reader who brought these errors to their attention.

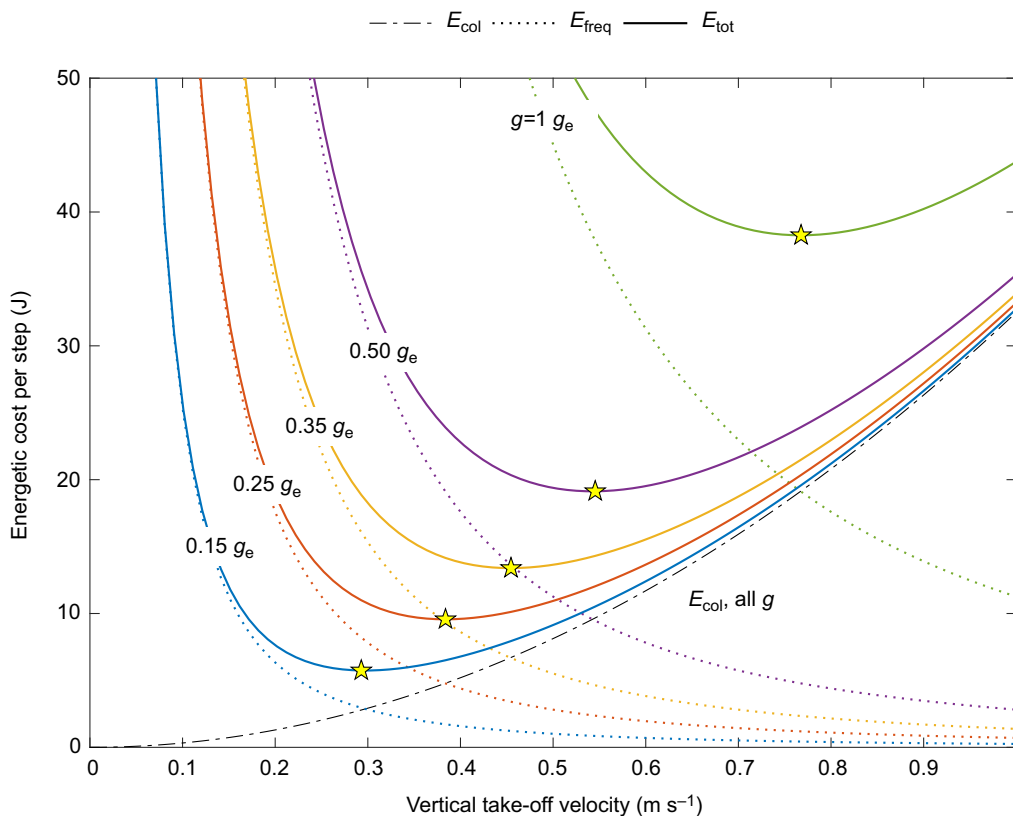


Fig. 4. The energetic costs according to the model are plotted as a function of vertical take-off velocity (V) for the five levels of gravity tested. The hypothetical subject has a mass of 65 kg and a frequency-based proportionality constant (A_2 in $E_{\text{freq}}=A_2f^2$) derived from the best fit in Fig. 2B. Labels of gravity levels (g) are placed over the colours they represent. The collisional cost curve ($E_{\text{col}}=mV^2/2$, black dot-dashed line) does not change with gravity, whereas the frequency-based energetic cost curve (E_{freq} , dotted lines) is sensitive to gravity, leading to an effect on total energy per step (E_{tot} , solid lines). In lower gravity, a runner can stay in the air longer for a given take-off velocity, so the associated frequency-based cost goes down. However, the cost of collisions at that same velocity is unchanged, because it depends only on the velocity itself. The relaxation of frequency-based cost allows the runner to settle on a lower optimal take-off velocity (yellow stars) with both a lower frequency-based and collisional cost, compared with higher gravity.

The authors apologise for any inconvenience this may have caused.

RESEARCH ARTICLE

Reducing gravity takes the bounce out of running

Delyle T. Polet^{1,*}, Ryan T. Schroeder² and John E. A. Bertram³

ABSTRACT

In gravity below Earth-normal, a person should be able to take higher leaps in running. We asked 10 subjects to run on a treadmill in five levels of simulated reduced gravity and optically tracked centre-of-mass kinematics. Subjects consistently reduced ballistic height compared with running in normal gravity. We explain this trend by considering the vertical take-off velocity (defined as maximum vertical velocity). Energetically optimal gaits should balance the energetic costs of ground-contact collisions (favouring lower take-off velocity), and step frequency penalties such as leg swing work (favouring higher take-off velocity, but less so in reduced gravity). Measured vertical take-off velocity scaled with the square root of gravitational acceleration, following energetic optimality predictions and explaining why ballistic height decreases in lower gravity. The success of work-based costs in predicting this behaviour challenges the notion that gait adaptation in reduced gravity results from an unloading of the stance phase. Only the relationship between take-off velocity and swing cost changes in reduced gravity; the energetic cost of the down-to-up transition for a given vertical take-off velocity does not change with gravity. Because lower gravity allows an elongated swing phase for a given take-off velocity, the motor control system can relax the vertical momentum change in the stance phase, thus reducing ballistic height, without great energetic penalty to leg swing work. Although it may seem counterintuitive, using less 'bouncy' gaits in reduced gravity is a strategy to reduce energetic costs, to which humans seem extremely sensitive.

KEY WORDS: Bipedal running, Reduced gravity, Leg swing, Energetics, Optimization, Biomechanics

INTRODUCTION

Under normal circumstances, why do humans and animals select particular steady gaits from the myriad possibilities available? One theory is that the chosen gaits minimize metabolic energy expenditure (Alexander and Jayes, 1983; Ruina et al., 2005). To test this theory, one can subject organisms to abnormal circumstances. If the gait changes to a new energetic optimum, it can be inferred that energetics also govern gait choice under normal conditions (Bertram and Ruina, 2001; Long and Srinivasan, 2013; Selinger et al., 2015).

One 'normal' gait is the bipedal run, and one abnormal circumstance is that of reduced gravity. Movie 1 demonstrates the profound effect reducing gravity has on running kinematics. A

representative subject runs at 2 m s^{-1} in both Earth-normal and simulated lunar gravity (approximately one-sixth of Earth-normal). The change in kinematics is apparent: the gait in normal gravity involves pronounced centre-of-mass undulations compared with the near-flat trajectory of the low-gravity gait. Although centre-of-mass vertical excursions during stance are known to decrease in reduced gravity (Donelan and Kram, 2000), we observed that the height achieved in the flight phase also decreases. This gait modification seems paradoxical: in reduced gravity, people are free to run with much higher leaps. Instead, they seem to flatten their gait. Why should this be?

A simple explanation posits that the behaviour is energetically beneficial. To explore the energetic consequences of choosing to run with lower leaps in reduced gravity, we first considered the impulsive model of running, following Rashevsky (1948) and Bekker (1962), which treats a human runner as a point mass body bouncing off rigid vertical limbs (Fig. 1). Stance is treated as an inelastic, impulsive collision with the ground. In reality, stance occurs in finite time, and elastic mechanisms exist. However, the inelastic approximation is remarkably productive in explaining gait choice (Ruina et al., 2005). When we use the term 'energetic cost of collisions', we are generally referring to non-recoverable energy loss during stance resulting from some interaction of the centre of mass with the ground (Bertram and Hasaneini, 2013). Such losses may arise from damping, active negative work or discontinuous velocity profiles. In any case, modelling these interactions as an inelastic collision provides a simple estimation of the net cost.

During this collision, all vertical velocity is lost while horizontal velocity is conserved (Fig. 1B). The total kinetic energy lost per step is therefore $E_{\text{col}} = mV^2/2$, where m is the runner's mass and V is their vertical take-off velocity. Lost energy must be recovered through muscular work to maintain a periodic gait, and so an energetically optimal gait will minimize these losses. If centre-of-mass kinetic energy loss were the only source of energetic cost, then the optimal solution would always be to minimize vertical take-off velocity. However, such a scenario would require an infinite stepping frequency as V approaches zero (Alexander, 1992; Ruina et al., 2005), as step frequency (ignoring stance time and air resistance) is $f = g/(2V)$, where g is gravitational acceleration.

Let us suppose there is an energetic penalty that scales with step frequency, as $E_{\text{freq}} \propto f^k \propto g^k/V^k$, where $k > 0$. Such a penalty may arise from work-based costs associated with swinging the leg, which are frequency dependent ($k=2$; Alexander, 1992; Doke et al., 2005), or from short muscle burst durations recruiting less efficient, fast-twitch muscle fibres ($k \approx 3$; Kram and Taylor, 1990; Kuo, 2001). Notably, this penalty increases with gravity, as the non-contact duration will be shorter for any given take-off velocity in higher gravity. The penalty also has minimal cost when V is maximal; smaller take-off velocities require more frequent steps, which is costly. Therefore, the two sources of cost act in opposite directions: collisional loss promotes lower take-off velocities, whereas frequency-based cost promotes higher take-off velocities.

¹Department of Biological Sciences, University of Calgary, Calgary, Canada, T2N 1N4. ²Biomedical Engineering Graduate Program, University of Calgary, Calgary, Canada, T2N 1N4. ³Cumming School of Medicine, University of Calgary, Calgary, Canada, T2N 1N4.

*Author for correspondence (dtpolet@ucalgary.ca)

 D.T.P., 0000-0002-8299-3434; J.E.A.B., 0000-0001-5943-7184

If these two effects are additive, then it follows that the total cost per step is:

$$E_{\text{tot}} = E_{\text{col}} + E_{\text{freq}} \quad (1)$$

$$= mV^2/2 + Ag^k/V^k,$$

where A is an unknown proportionality constant relating frequency to energetic cost. As the function is continuous and smooth for $V > 0$, a minimum can only occur either at the boundaries of the domain, or when $\frac{\partial E_{\text{tot}}}{\partial V} = 0$. Solving the latter equation for V yields:

$$V^* \propto g^{k/(k+2)} \quad (2)$$

as the unique critical value. Here the asterisk denotes a predicted (optimal) value. Because E_{tot} approaches infinity as V approaches 0 and infinity (Eqn 1), the critical value must be the global minimum in the domain $V > 0$. As $k > 0$, it follows from Eqn 2 that the energetically optimal solution is to reduce the vertical take-off velocity as gravity decreases.

The observation of He et al. (1991) that $V \propto \sqrt{g}$ implies $k=2$, a finding consistent with frequency costs arising from the work of swinging the limb (Alexander, 1992; Doke et al., 2005). In reality, He et al. (1991) measured vertical speed at initial foot contact, but for the impulsive model in its simplest form, this is indistinguishable from take-off velocity. Their empirical assessment of the relationship used a small sample size, with only four subjects. We tested the prediction of Eqn 2 by measuring the take-off velocity over each running stride in 10 subjects using a harness that simulates reduced gravity. [In this paper, we are taking the vertical take-off velocity as the maximum vertical velocity during the gait cycle, following Cavagna (2006).] We also measured the maximum vertical displacement in the ballistic phase to verify whether the counterintuitive observation of lowered ballistic centre-of-mass

List of symbols

A	proportionality constant in the relationship $E_{\text{freq}} = Af^k$ (J s ^k)
B	proportionality constant in the relationship $E_{\text{swing}} = Bml^2(f^2 - f_n^2)$
E_{col}	energetic cost of collisions (J)
E_{freq}	energetic cost related to step-frequency (J)
E_{swing}	energetic cost of leg swing work (J)
E_{tot}	total energetic cost ($E_{\text{col}} + E_{\text{freq}}$ or $E_{\text{col}} + E_{\text{swing}}$, in J)
f	step frequency (Hz)
f_n	natural pendular frequency (Hz)
g	gravitational acceleration (m s ⁻²)
g_e	Earth-normal gravitational acceleration (9.8 m s ⁻²)
Gr	Groucho number ($\equiv v\omega_0/g$)
H	ballistic height (m)
I	leg moment of inertia about the hip (kg m ²)
k	exponent in proportionality ($E_{\text{freq}} \propto f^k$)
l	leg length (m)
m	total subject mass (kg)
r	leg length change from rest length (m)
t	time after toe-down (s)
t^*	time at which maximum vertical speed is achieved (s)
t_m	time at which maximum vertical velocity is achieved (s)
t_s	stance period (s)
U	average horizontal speed (m s ⁻¹)
v	vertical velocity at toe-off (m s ⁻¹)
V	vertical velocity at take-off (maximum vertical velocity, in m s ⁻¹)
V^*	predicted (optimal) vertical take-off velocity (m s ⁻¹)
θ	leg angle (rad)
ω_0	vertical natural angular frequency in the spring-mass model (rad s ⁻¹)

height in hypogravity, as exemplified in Movie 1, is a consistent feature of reduced-gravity running.

MATERIALS AND METHODS

We asked 10 healthy subjects to run on a treadmill for 2 min at 2 m s⁻¹ in five different gravity levels (0.15, 0.25, 0.35, 0.50 and 1.00 g_e ,

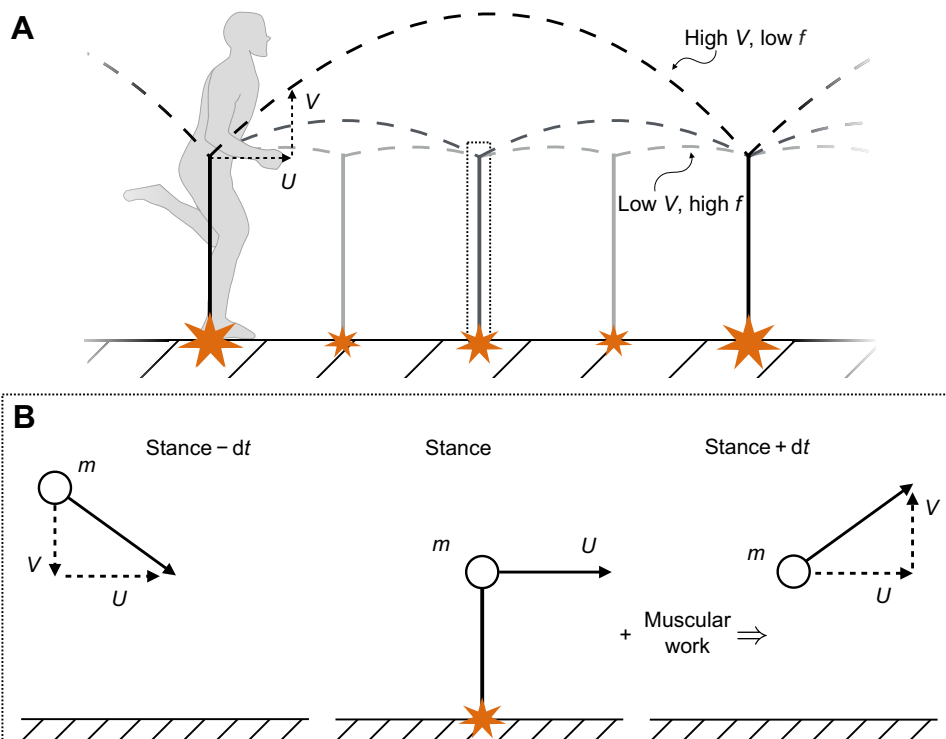


Fig. 1. Schematics explaining the energetic model. (A) In the impulsive model of running, a point mass bounces off vertical, massless legs during an infinitesimal stance phase. As the horizontal velocity U is conserved, the vertical take-off velocity V dictates the step frequency and stride length. Smaller take-off velocities (light grey) result in more frequent steps that incur an energetic penalty, while larger take-off velocities (dark grey) reduce the frequency penalty but increase losses during stance. The dotted outline represents a short time around stance that is expanded in B. (B) We assume that the centre-of-mass speed at landing is equal to the take-off speed. The vertical velocity V and its associated kinetic energy are lost during an impulsive foot-ground collision of infinitesimally short duration. The lost energy must be resupplied through muscular work. Horizontal acceleration is assumed to be small and is neglected in the model. m is body mass and dt is a short time step.

where g_e is 9.8 m s^{-2}). A belt speed of 2 m s^{-1} was chosen as a comfortable, intermediate jogging pace that could be accomplished at all gravity levels. Reduced gravities were simulated using a harness-pulley system similar to that used by Donelan and Kram (2000), but differing in the use of a spring-pendulum system to generate near-constant force for a large range of motion. Hasaneini et al. (2017 preprint) provide more details of the apparatus. The University of Calgary Research Ethics Board approved the study protocol and written informed consent was obtained from all subjects. Leg length for each subject was measured during standing from the base of the shoe to the greater trochanter on one leg.

Owing to the unusual experience of running in reduced gravity, subjects were allowed to acclimate at their leisure before indicating they were ready to begin each 2-min measurement trial. In each case, the subject was asked simply to run in any way that felt comfortable. Data from 30 to 90 s from trial start were analyzed, providing a buffer between acclimating to experimental conditions at trial start and initiating slowdown at trial end.

Implementation and measurement of reduced gravity

Gravity levels were chosen to span a broad range. Of particular interest were low gravities, at which the model predicts unusual body trajectories. Thus, low levels of gravity were sampled more thoroughly than others. The order in which gravity levels were tested was randomized for each subject, so as to minimize sequence conditioning effects.

For each gravity condition, the simulated gravity system was adjusted in order to modulate the force pulling upward on the subject. In this particular harness, variations in spring force caused by support-spring stretch during cyclic loading over the stride were virtually eliminated using an intervening lever (see figs 3 and 4 in Hasaneini et al., 2017 preprint). The lever moment arm was adjusted in order to set the upward force applied to the harness, and was calibrated with a known set of weights prior to all data collection. A linear interpolation of the calibration was used to determine the moment arm necessary to achieve the desired upward force, given the subject weight and targeted effective gravity. Using this system, the standard deviation of the upward force during a trial (averaged across all trials) was 3% of the subject's Earth-normal body weight.

Achieving exact target gravity levels was not possible because the lever's moment arm is limited by discrete force increments (approximately 15 N). Thus, each subject received a slight variation of the targeted gravity conditions, depending on their weight. A real-time data acquisition system allowed us to measure tension forces at the gravity harness and calculate the effective gravity level at the beginning of each new condition. The force-sensing system consisted of an analog strain gauge (Micro-Measurements CEA-06-125UW-350, Wendell, NC, USA), mounted to a C-shaped steel hook connecting the tensioned cable and harness. The strain gauge signal was passed to a strain conditioning amplifier (National Instruments SCXI-1000 amp with SCXI-1520 eight-channel universal strain gauge module connected with SCXI-1314 terminal block, Austin, TX, USA), digitized (NI-USB-6251 mass termination) and acquired in a custom virtual instrument in LabVIEW (National Instruments). The tension transducer was calibrated with a known set of weights once before and once after each data collection trial to correct for modest drift error in the signal. The calibration used was the mean of the pre- and post-experiment calibrations.

Centre of mass kinematic measurements

A marker was placed at the lumbar region of the subject's back, approximating the position of the centre of mass. Each trial was

filmed at 120 Hz using a Casio EX-ZR700 digital camera (Casio Computer Co., Ltd, Shibuya, Tokyo, Japan). The marker position was digitized in DLTdv5 (Hedrick, 2008). Position data were differentiated using a central differencing scheme to generate velocity profiles, which were further processed with a fourth-order low-pass Butterworth filter at 7 Hz cut-off. The vertical take-off velocity was defined as the maximum vertical velocity during each gait cycle (V in Fig. 1). This definition corresponds to the moment at the end of stance where the net vertical force on the body is null, in accordance with a definition of take-off proposed by Cavagna (2006).

Vertical take-off velocities were identified as local maxima in the vertical velocity profile. Filtering and differentiation errors occasionally resulted in some erroneous maxima being identified. To rectify this, first any maxima within 10 time steps of data boundaries were rejected. Second, the stride period was measured as time between adjacent maxima. If any stride period was 25% lower than the median stride period or less, the maxima corresponding to that stride period were compared and the largest maximum was kept, with the other being rejected. This process was repeated until no outliers remained.

Position data used to determine ballistic height were processed with a fourth-order low-pass Butterworth filter at 9 Hz cut-off. Ballistic height was defined as the vertical displacement from take-off to the maximum height within each stride. No outlier rejection was used to eliminate vertical position data peaks, as the filtering was slight and no differentiation was required. If a take-off could not be identified prior to the point of maximum height within half the median stride time, the associated measurement of ballistic height was rejected; this strategy prevented peaks from being associated with take-off from a different stride.

Statistical methods

Take-off velocities and ballistic heights were averaged across all gait cycles in each trial for each subject. To test whether ballistic height varied with gravity, a linear model between ballistic height and gravitational acceleration was fitted to the data using least-squares regression, and the validity of the fit was assessed using an F -test. A linear model was also tested for $\log(V)$ against $\log(g)$ using the same methods. Because the proportionality coefficient between V^* and \sqrt{g} is unknown *a priori*, we derived its value from a least-squares best fit of measured vertical take-off velocity against the square root of gravitational acceleration, setting the intercept to zero. Given a minimal correlation coefficient of 0.5 and sample size of 50, a *post hoc* power analysis yields statistical power of 0.96, with type I error margin of 0.05. Data were analyzed using custom scripts written in MATLAB (v. 2016b, MathWorks, Natick, MA, USA).

RESULTS

Response of ballistic height and take-off velocity to gravity

Data from all trials are shown in Fig. 2. Ballistic height increases with gravity (linear versus constant model, $P=4 \times 10^{-4}$, $R^2=0.24$, $N=50$; Fig. 2A), validating the counterintuitive result exemplified in Movie 1 as a consistent feature of running in hypogravity.

Take-off velocity also increases with gravitational acceleration (Fig. 2B), and a least-squares fit of Eqn 2 using $k=2$ follows empirical measurements well ($R^2=0.73$, $N=50$). Other values of k were also tested (Fig. 3). If the impulsive model is accurate, then the best-fit slope of a scatter plot of $\log(V)$ against $\log(g)$ should correspond to $k/(k+2)$ (Eqn 2), that is, slopes of 0.33, 0.50 or 0.60 for $k=1, 2$ and 3, respectively. Only the slope predicted by $k=2$

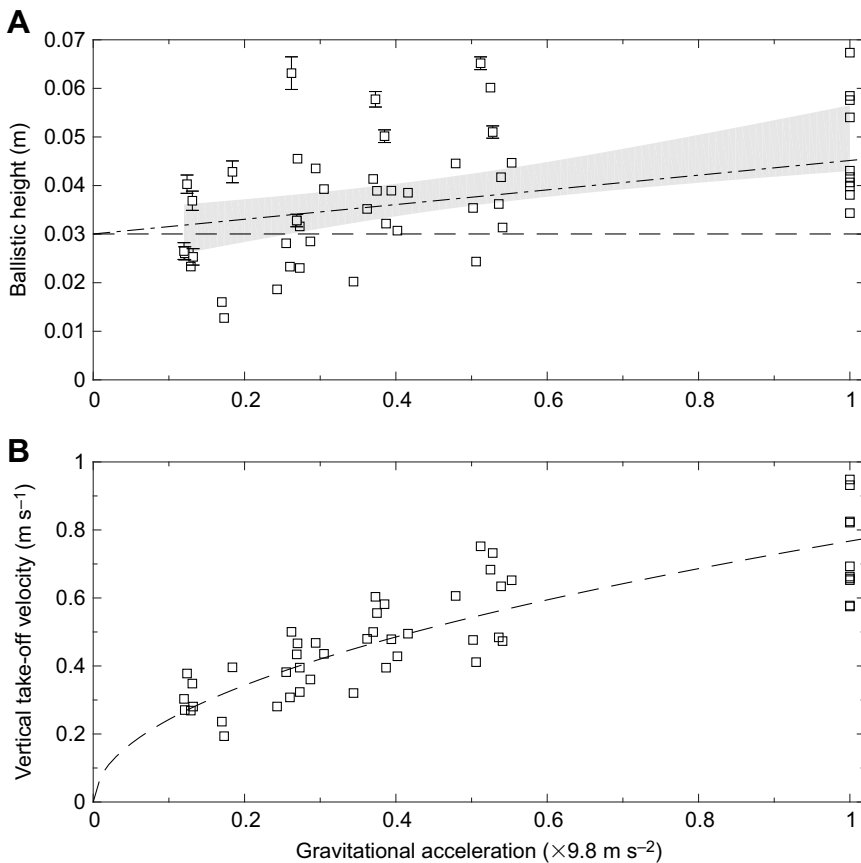


Fig. 2. Human subjects lower both ballistic height and take-off velocity during running in reduced gravity. (A) Mean ballistic height (data points) increases with gravity (linear versus constant model under two-tailed F -test, $P=4\times 10^{-4}$, $N=50$). The dashed line is the prediction for ballistic height from the impulsive model, which deviates from observation at high g . The dot-dashed line adds a correction factor for finite stance time from the spring-mass model (Eqn 3). This second prediction lies within the 95% confidence intervals (CI) of the least-squares linear fit (grey area). Both predictions use take-off velocities from the best fit in B. (B) Measured vertical take-off velocities increase proportionally with the square root of gravitational acceleration, following work-based energetic optimality. The least squares fit of the impulsive model with $k=2$ is shown as a dashed line. The fit has an R^2 value of 0.73 ($N=50$). For both panels, each data point is a mean value measured in one subject (10 subjects total) across multiple steps ($n\geq 50$) during a 1-min period at a given gravity level. If error bars (twice the s.e.m.) are smaller than the markers, then they are not shown. Data used for creating these graphics are given in Table S1.

falls within the 95% confidence interval of the least squares slope (0.47 ± 0.09 ; Fig. 3).

A best fit at $k=2$ implies a frequency-based cost arising primarily from the work of leg swing. However, because only the centre of mass is offloaded by the harness, the natural frequency of limb

swing remains unchanged for all target gravity levels (Donelan and Kram, 2000). Because metabolic energy of swing is minimal at natural frequency (Doke et al., 2005), it is necessary to adjust the predictions from the impulsive model (Appendix 1). An adjusted model exhibits a fit with $R^2=0.745$ ($N=50$; Fig. A1), only

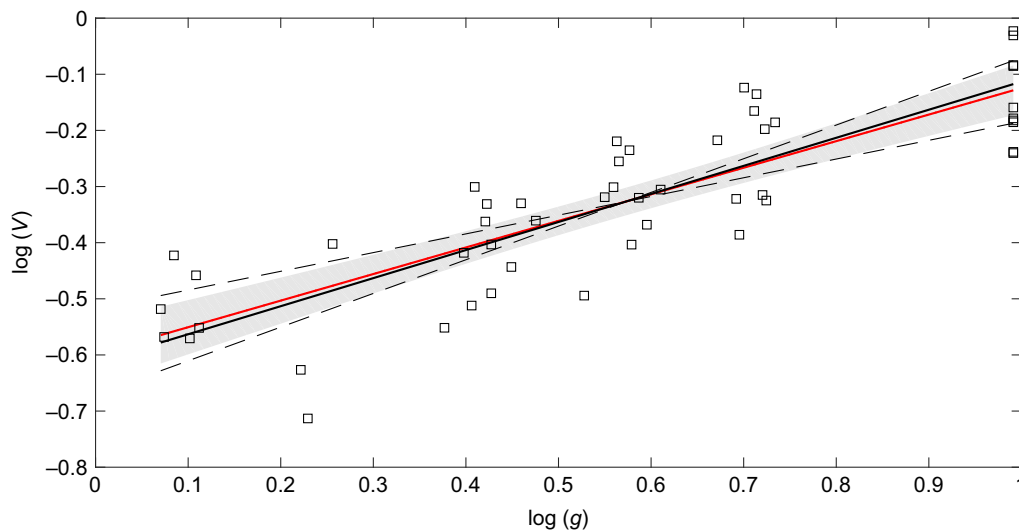


Fig. 3. A log-log plot of vertical take-off velocity against gravitational acceleration shows that the impulsive model yields the best fit when $E_{\text{freq}}\propto f^2$. The least-squares linear fit is shown in red as a solid line, with 95% CI as a grey area. The linear fit exhibits $R^2=0.70$ and a slope of 0.47 ± 0.09 (best estimate $\pm 95\%$ CI, $N=50$), which is not significantly different from the predicted slope of 0.5 for $k=2$ (black solid line), where k is the exponent relating frequency to cost ($E_{\text{freq}}\propto f^k$). Both $k=1$ and $k=3$ (shallow and steep dashed lines, respectively) yield predicted slopes (0.33 and 0.60, respectively) that lie outside the 95% CI, indicating that a work-based swing cost at $k=2$ is a superior fit to the data, while a simple linear frequency cost ($k=1$) and an approximate force/time cost ($k=3$; see Kuo, 2001) do not represent these data well. Data points are from 10 subjects running at five gravity conditions each, and each point is the mean of at least 64 take-offs measured during each trial.

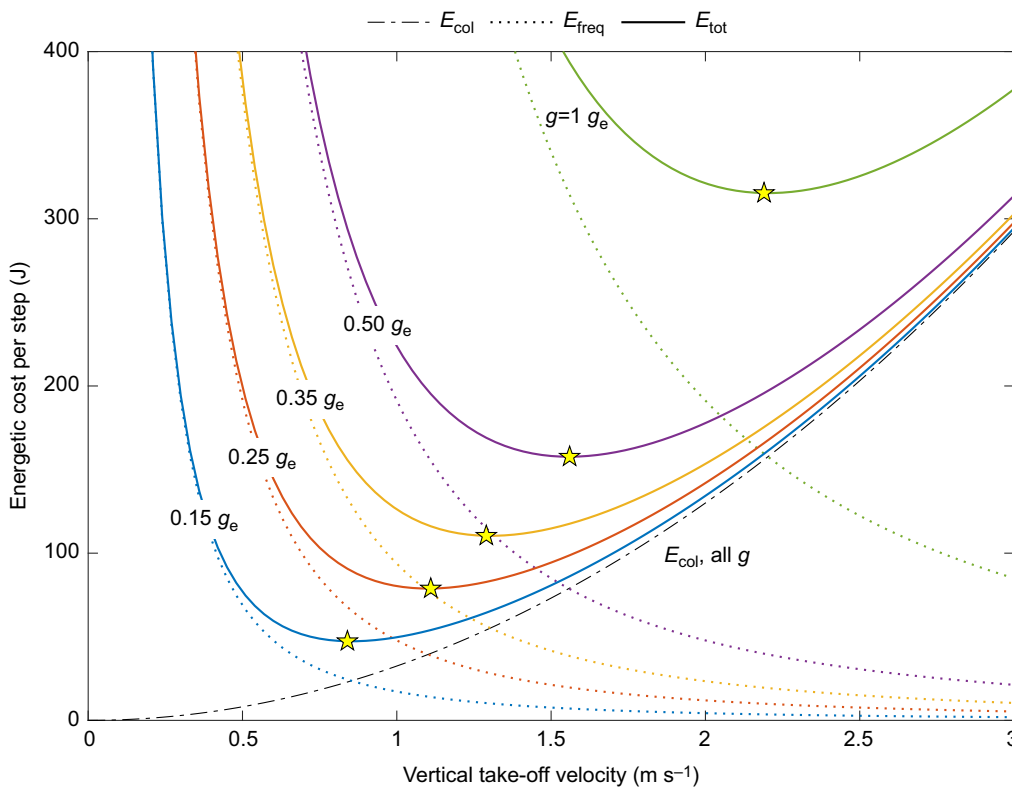


Fig. 4. The energetic costs according to the model are plotted as a function of vertical take-off velocity (V) for the five levels of gravity tested. The hypothetical subject has a mass of 65 kg and a frequency-based proportionality constant (A in $E_{\text{freq}}=Af^2$) derived from the best fit in Fig. 2B. Labels of gravity levels (g) are placed over the colours they represent. The collisional cost curve ($E_{\text{col}}=mV^2/2$, black dot-dashed line) does not change with gravity, whereas the frequency-based energetic cost curve (E_{freq} , dotted lines) is sensitive to gravity, leading to an effect on total energy per step (E_{tot} , solid lines). In lower gravity, a runner can stay in the air longer for a given take-off velocity, so the associated frequency-based cost goes down. However, the cost of collisions at that same velocity is unchanged, because it depends only on the velocity itself. The relaxation of frequency-based cost allows the runner to settle on a lower optimal take-off velocity (yellow stars) with both a lower frequency-based and collisional cost, compared with higher gravity.

marginally better than the simple model with $k=2$ ($R^2=0.73$; Fig. 2B). The predictions do not change greatly, because time spent in the air is affected by gravity, and more air time requires less work to swing the legs, regardless of natural frequency [as long as stride frequency is greater than natural frequency, which is very likely the case for the present study (Appendix 1)].

Predicting ballistic height trends

The impulsive model with $k=2$ predicts that the ballistic height should remain constant (dashed line in Fig. 2A). This constant value agrees with empirical data at low g , but exhibits increasing error towards Earth-normal g .

We defined ‘take-off’ as occurring when the net force on the body was null and velocity was maximal; however, this does not equate to the moment when the stance foot leaves the ground. After the point of maximal velocity, upward ground reaction forces decay to zero. During this time, the net downward acceleration on the body is less than gravitational acceleration. Thus, the body travels higher than would be expected if maximal velocity corresponded exactly to the point where the body entered a true ballistic phase, as in the model (Fig. 1).

We can account for the missing impulse with the spring-mass model. This model describes the kinematics and dynamics of running well (McMahon and Cheng, 1990; He et al., 1991; Blickhan and Full, 1993), and provides a way to estimate stance time from take-off velocity (though it lacks the ability to predict take-off velocity; McMahon and Cheng, 1990). Notably, correcting the prediction $V \propto \sqrt{g}$ with spring-mass model estimates of finite stance yields the following relationship for ballistic height (Appendix 2):

$$H = \frac{g}{2\omega_0^2} + \frac{A^2}{2}, \quad (3)$$

where ω_0 is the natural angular frequency of vertical oscillation, and A is a constant in the relationship $V = A\sqrt{g}$. Note that Eqn 3 is linear in

g , and approaches the predictions from the impulsive model alone as $g \rightarrow 0$. Taking $\omega_0=18 \text{ rad s}^{-1}$ from He et al. (1991), and A from the best-fit in Fig. 2B, Eqn 3 gives the dot-dashed line shown in Fig. 2A. The predicted relationship (Eqn 3) has a slope of 0.015 m g_e^{-1} and an intercept of 0.03 m , and is within the 95% confidence interval of the best-fit slope ($0.021 \pm 0.01 \text{ m g}_e^{-1}$) and intercept ($0.029 \pm 0.006 \text{ m}$), indicating that finite stance accounts for the discrepancy within error, though it somewhat underpredicts the true slope.

DISCUSSION

Human runners lower the height achieved in the ballistic phase as gravity decreases. This adaptation requires pronounced modification of the take-off velocity, as maintaining the latter parameter in all conditions would result in substantially increased ballistic height in reduced gravity. Why human runners would modify their gait so greatly was initially unclear.

A simple work-based model of energetic cost explains the trends well. The fit in Fig. 2B exhibits an R^2 value of 0.73, indicating that a simple energetic model can explain over two-thirds of the variation in maximum vertical velocity resulting from changes in gravity. Human runners seem to be sensitive to these energetic costs and adjust their take-off velocity accordingly. However, the model has its limitations, and an accounting of finite stance (which was initially neglected in the model) was necessary to explain the trend of increasing ballistic height with gravity. Despite the updated model matching the general trend of the data, the slope in Eqn 3 is reduced compared with the empirically derived slope.

The use of the external lumbar point as a centre of mass approximation may explain some of the remaining difference between Eqn 3 and observation. At lower gravity, the body maintained a relatively erect, rigid posture (as exemplified by Movie 1), and so the lumbar marker likely follows the centre of mass closely. However, at higher gravity, the legs move through larger

excursions and the torso exhibits slight rotation, making the lumbar estimate less accurate. At normal gravity, Slawinski et al. (2004) showed that the lumbar point overestimates vertical oscillations of the flight phase (by less than 1 cm), though their trials were at a high belt speed (5 m s^{-1}). If the same results hold in our case, we would expect that the measured ballistic height in Fig. 2A should be slightly lower at higher levels of gravity, reducing the actual slope and possibly improving the agreement to Eqn 3. Future work could use a multisegment model to improve centre of mass and ballistic height measurements, but such a technique is unlikely to reverse the trend of increasing ballistic height with gravitational acceleration.

The present results indicate that the cost of step frequency is a key factor in locomotion. Although the exact value of the optimal take-off velocity depends on both frequency-based penalties and collisional costs, the former penalties change with gravity while the latter do not (Fig. 4). The collisional cost landscape is independent of gravity because the final vertical landing velocity is alone responsible for the lost energy. Regardless of gravitational acceleration, vertical landing speed must equal vertical take-off speed in the model, so a particular take-off velocity will have a particular, unchanging collisional cost.

However, taking off at a particular vertical velocity results in greater flight time at lower levels of gravity; thus, the frequency-based cost curves are decreased as gravity decreases (Fig. 4). Frequency-based costs, particularly limb-swing work, appear to be an important determinant of the effective movement strategies available to the motor control system. Their apparent influence warrants further investigation into the extent of their contribution to metabolic expenditure.

Although the present study corroborates others in finding that a work-based cost ($k=2$) predicts locomotion well (Alexander, 1980, 1992, Hasaneini et al., 2013), other authors have favoured a higher-order ‘force/time’ cost (Kuo, 2001; Doke et al., 2005; Doke and Kuo, 2007). Interestingly, a higher-order model in frequency cost ($k=3$) did not fit the present data; however, our simple model with $k=3$ only approximates the force/time cost in the swing phase, and does not account for a rate cost during stance. Further research must be done to distinguish the predictive value of work-based cost to its alternatives; however, for the present results, a work-based model is sufficient, at least for take-off velocity.

The present results challenge the notion that metabolic cost of running is determined largely by the cost of generating force during stance (Kram and Taylor, 1990; Arellano and Kram, 2014), purportedly supported by the observation that metabolic cost is proportional to gravity (Farley and McMahon, 1992). According to the best-fit model presented here, the net cost (Eqn 1) at optimal take-off velocity (Eqn 2) is expected to increase in proportion to gravitational acceleration [that is, $E_{\text{tot}}(V^*) \propto g$], as Farley and McMahon (1992) observed. The cost of vertical acceleration of the centre of mass can decrease as gravity is reduced only because the relationship between take-off velocity and swing cost changes; this allows the subject to settle on a lower stance cost, whose relationship to take-off velocity does not change as a function of gravity (Fig. 4). These trends can be explained simply from muscular work, and do not rely on any independent force-magnitude cost.

The model presented in this article is admittedly simple and makes unrealistic assumptions, including impulsive stance, no horizontal muscular force, non-distributed mass, and a simple relationship between step frequency and energetic cost. Further, horizontal accelerations will incur a larger portion of energetic losses as horizontal speed increases (Willems et al., 1995), and the trade-off

between swing and stance costs may change. The present model would not be able to anticipate any such trend, as it has no dependence on horizontal speed. Future investigations could evaluate work-based costs using more advanced optimal control models (Srinivasan and Ruina, 2006; Hasaneini et al., 2013), eliminating some of these assumptions and allowing for an investigation into horizontal speed dependence. Despite its simplicity, the impulsive model with work-based swing cost is able to correctly predict the observed trends in take-off velocity with gravity, and demonstrates that understanding the energetic cost of both swing and stance is crucial to evaluating why the central nervous system selects specific running motions in different circumstances.

Although many running conditions are quite familiar, running in reduced gravity is outside our general experience. Surprisingly, releasing an individual from the downward force of gravity does not result in higher leaps between foot contacts. Rather, humans use less bouncy gaits with slow take-off velocities in reduced gravity, taking advantage of a reduced collisional cost while balancing a stride-frequency penalty.

APPENDIX 1

Cost of swing work in partial reduced gravity

The experimental apparatus (Hasaneini et al., 2017 preprint) unloads a subject’s centre of mass, but does not act directly on their limbs. Consequently, while their centre of mass might experience reduced weight, the limbs swing under the influence of normal gravity. It is prudent to check how this affects the predictions of the impulsive model.

The work required to swing a limb is (Doke et al., 2005):

$$E_{\text{swing}} \propto I(f^2 - f_n^2), \quad (\text{A1})$$

where I is the moment of inertia of the limb about the hip, f is the frequency of oscillation and f_n is the natural frequency (equal to $\sqrt{g/l}$ for a simple pendulum, where l is leg length). Here we are assuming that the limb changes configuration little during the swing phase, and so I is approximately constant. Note that Eqn A1 is only valid when $f > f_n$ (Doke et al., 2005), because if sufficient time is available the limb can swing passively. The swing frequency is slightly greater than the stride frequency (swing period is two flight phases and one stance phase, or one stance phase shorter than stride period), which in the present study ranged from trial-mean values of 0.69 to 1.47 Hz over all subjects and conditions (Table S1). Doke et al. (2005) found the natural frequency of swinging legs to be 0.64 ± 0.02 Hz (mean \pm s.d.) for a subject group with mean leg length of 0.88 ± 0.07 m ($N=12$). Our subject group exhibited larger mean leg length (0.92 ± 0.06 m, $N=10$), so would very likely have smaller natural frequencies. Therefore, the assumption that $f > f_n$ very likely holds in this case.

The leg moment of inertia about the hip scales approximately as $I \propto ml^2$, where m is body mass and l is leg length (Winter, 2009). Assuming $f = g/(2V)$, and invoking $E_{\text{tot}} = E_{\text{col}} + E_{\text{swing}}$, we have:

$$E_{\text{tot}} = mV^2/2 + Bml^2 \left(\left(\frac{g}{2V} \right)^2 - f_n^2 \right), \quad (\text{A2})$$

where B is some proportionality constant. To achieve the energetically optimal take-off velocity, we take the derivative of Eqn A2 with respect to V , yielding:

$$\left. \frac{\partial E_{\text{tot}}}{\partial V} \right|_{V=V^*} = mV^* - Bml^2 \frac{g^2}{2(V^*)^3} = 0, \quad (\text{A3})$$

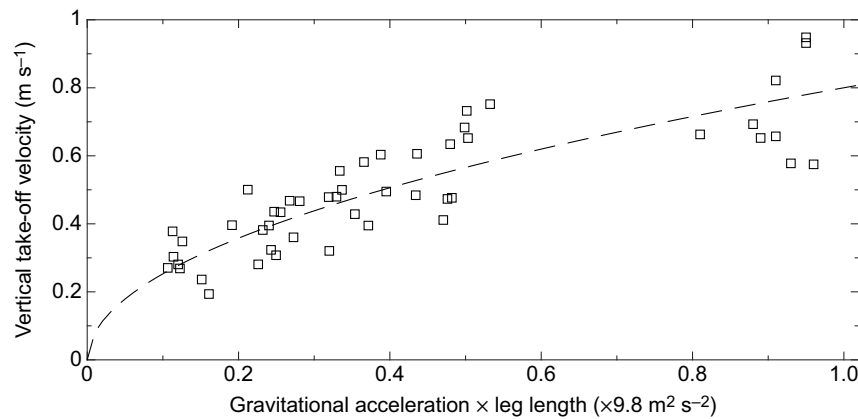


Fig. A1. Vertical take-off velocity scales with the square root of gravitational acceleration times leg length during running. The least-squares fit for the model given by Eqn A4 is shown as a dashed line. The fit exhibits $R^2=0.745$, using all 50 data points. Error bars (twice standard error of the mean take-off velocity measured during a trial, $n \geq 64$) are smaller than the marker size.

where we note that any dependence on f_n has disappeared. However, there is a new dependence on l . Solving Eqn A3 for V^* , we find:

$$V^* \propto \sqrt{gl}. \quad (\text{A4})$$

Empirical V is plotted against gl in Fig. A1 with the least-square fit of Eqn A4. The fit exhibits $R^2=0.745$, only a slight improvement compared with the simple impulsive model ($R^2=0.73$). Eqn A4 depends on l , but if the variation in l is small, then Eqn A4 is indistinguishable from the simple swing-cost model (Eqn 2 with $k=2$). Indeed, the leg lengths of our subject group varied only by a factor of 1.3 (range 0.81 to 1.04 m), while the highest experimental g was six times the smallest value. Because the variation in leg length is comparatively small, it has little impact on the results.

APPENDIX 2

Ballistic height corrections from the spring-mass model

We seek to predict the vertical centre-of-mass displacement achieved between take-off (maximum vertical velocity) and the maximum height during the flight phase. The vertical displacement from toe-off is $v^2/(2g)$, where v is the vertical velocity at toe-off. However, we do not know the displacement between take-off and toe-off, nor do we know how to relate the velocity at take-off to the velocity at toe-off. Both of these unknowns could be calculated using the ground reaction force during stance, but this was not measured empirically.

Instead, we can rely on the spring-mass model, which gives a decent approximation of the ground reaction forces assuming the velocity at toe-off and natural angular frequency (ω_0) are given (McMahon and Cheng, 1990). In our case, the toe-off velocity is unknown, but the spring-mass model allows us to relate it to the maximum vertical velocity, which can in turn be predicted by the impulsive model. ω_0 is defined as $\sqrt{k/m}$, where k is the 'spring' stiffness and m is mass. k is not actually the tendon stiffness, but is the virtual stiffness generated by the motor control system during stance (Farley and Ferris, 1998; Donelan and Kram, 2000); that is, the muscle and tendon forces combine to generate ground reaction forces as if there were one linear spring acting on the centre of mass. The complicated interplay between muscles, tendons and energetics makes the angular frequency hard to predict.

Fortunately, the vertical spring stiffness is held more-or-less constant through changes in gravity (He et al., 1991), so we can use the empirically derived value of $\omega_0 \sim 18 \text{ rad s}^{-1}$. It remains simply to find the displacement between take-off and toe-off, and the vertical toe-off velocity, in terms of the vertical take-off velocity and gravity.

[The value of ω_0 was calculated by taking the average value of vertical stiffness data in fig. 7 of He et al. (1991), dividing by average subject mass from the same study and taking the square root. $\omega_0=18 \text{ rad s}^{-1}$ falls within all the error bars of fig. 7, and so seems representative of the natural angular frequency at all levels of gravity.]

We follow McMahon and Cheng (1990) in assuming a point-mass body of mass m and massless legs. We assume that the ground reaction force is well approximated by the compression of a spring with angular frequency ω_0 . For simplicity, we use a hopping model, which assumes that a person exhibits a small excursion angle (i.e. $\theta \sim 0$). The leg length minus resting length is r , and so the dynamics of the system are:

$$\ddot{r} + \omega_0^2 r + g = 0. \quad (\text{A5})$$

Setting the vertical landing velocity to $\dot{r}(0)=-v$, and the initial position as $r(0)=0$, the solution to the ordinary differential equation is (McMahon and Cheng, 1990):

$$\omega_0^2 r(t) = -\omega_0 v \sin(\omega_0 t) + g \cos(\omega_0 t) - g. \quad (\text{A6})$$

The instantaneous velocity is thus:

$$\dot{r} = -v \cos(\omega_0 t) - \frac{g}{\omega_0} \sin(\omega_0 t). \quad (\text{A7})$$

Eqns A5–A7 are valid for $0 \leq t \leq t_s$, where $t_s = [2\pi - 2\arctan(Gr)]/\omega_0$ is the stance period, and we have introduced the non-dimensional Groucho number $Gr = v\omega_0/g$ (McMahon and Cheng, 1990). For $t_s < t < t_s + 2v/g$, the body is in a ballistic phase.

We can now determine the timing and magnitude of the peak vertical velocity. Let t^* correspond to any time at which a maximum speed is achieved. Because Eqn A7 is smooth and periodic, local maxima and minima in velocity must satisfy $\ddot{r} = 0$. Therefore, from Eqn A5:

$$r(t^*) = -\frac{g}{\omega_0^2}. \quad (\text{A8})$$

Combining Eqn A8 with A6 and solving for $0 \leq t^* \leq t_s$ yields:

$$t^* = [\arctan(Gr^{-1}) + n\pi]/\omega_0, \quad n = 0, 1, \quad (\text{A9})$$

corresponding to the points of maximal speed during stance. The second point ($n=1$), corresponds to the time at which maximal velocity is achieved:

$$t_m = (\arctan(Gr^{-1}) + \pi)/\omega_0. \quad (\text{A10})$$

To determine the peak velocity V , we insert Eqn A10 into A7. Using the relationships $\cos(\arctan(x))=1/\sqrt{x^2+1}$ and $\sin(\arctan(x))=x/\sqrt{x^2+1}$, we find:

$$V = \frac{g}{\omega_0} \sqrt{Gr^2 + 1} \quad \text{and} \quad (\text{A11})$$

$$v^2 = V^2 - (g/\omega_0)^2. \quad (\text{A12})$$

In the main text, we define the ballistic height (H) as the vertical displacement from the time of maximal vertical velocity to the maximum height achieved during a stride, that is:

$$H = \frac{v^2}{2g} - r(t_m). \quad (\text{A13})$$

We need only insert Eqns A8 and A12 into Eqn A13 to find:

$$H = \frac{V^2}{2g} + \frac{g}{2\omega_0^2}. \quad (\text{A14})$$

Note that the first term is identical to the prediction of the impulsive model (i.e. $V=v$), while the second term gives a correction from the spring mass model, due to finite stance time. Because we have established that $V=A\sqrt{g}$, the prediction for H in terms of g alone is:

$$H(g) = \frac{A^2}{2} + \frac{g}{2\omega_0^2}. \quad (\text{A15})$$

Acknowledgements

We thank Art Kuo, Jim Usherwood, David Lee and Allison Smith for comments on earlier drafts, as well as two anonymous reviewers, who provided constructive insights that greatly improved the manuscript.

Competing interests

The authors declare no competing or financial interests.

Author contributions

Conceptualization: D.T.P., R.T.S., J.E.A.B.; Methodology: D.T.P., R.T.S., J.E.A.B.; Software: D.T.P., R.T.S.; Formal analysis: D.T.P.; Investigation: D.T.P., R.T.S., J.E.A.B.; Resources: J.E.A.B.; Data curation: D.T.P., R.T.S.; Writing - original draft: D.T.P.; Writing - review & editing: D.T.P., R.T.S., J.E.A.B.; Visualization: D.T.P.; Supervision: J.E.A.B.; Project administration: D.T.P., R.T.S., J.E.A.B.; Funding acquisition: D.T.P., J.E.A.B.

Funding

This work was funded by the Natural Sciences and Engineering Research Council of Canada [CGSD3-459978-2014 to D.T.P., 312117-2012 to J.E.A.B.].

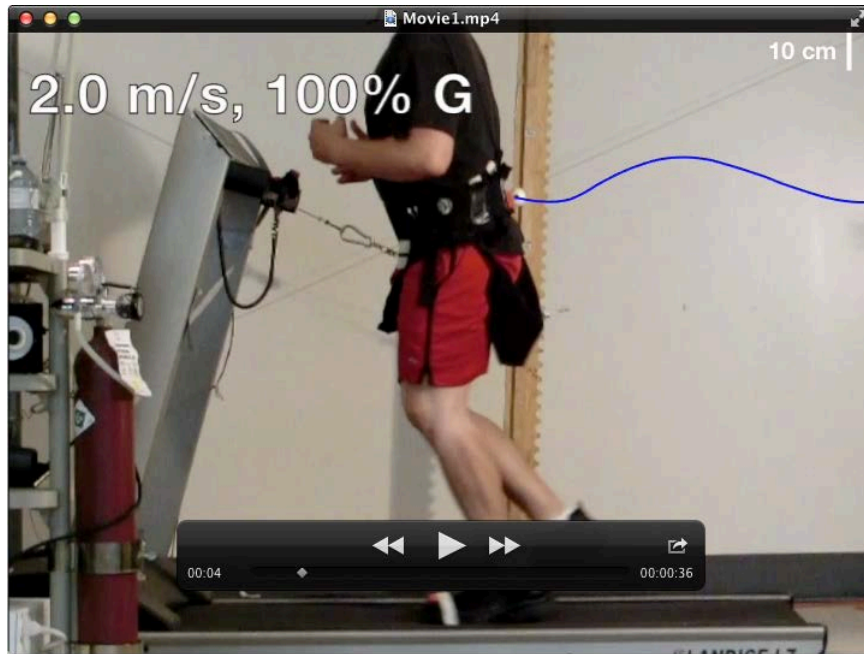
Supplementary information

Supplementary information available online at <http://jeb.biologists.org/lookup/doi/10.1242/jeb.162024.supplemental>

References

Alexander, R. M. N. (1980). Optimum walking techniques for quadrupeds and bipeds. *J. Zool.* **192**, 97-117.

- Alexander, R. M. N. (1992). A model of bipedal locomotion on compliant legs. *Philos. Trans. R. Soc. Lond. B Biol. Sci.* **338**, 189-198.
- Alexander, R. M. N. and Jayes, A. S. (1983). A dynamic similarity hypothesis for the gaits of quadrupedal mammals. *J. Zool.* **201**, 135-152.
- Arellano, C. J. and Kram, R. (2014). Partitioning the metabolic cost of human running: a task-by-task approach. *Integr. Comp. Biol.* **54**, 1084-1098.
- Bekker, M. G. (1962). Locomotion in nature. In *Theory of Land Locomotion*, 2nd edn, pp. 4-26. Ann Arbor, MI: University of Michigan Press.
- Bertram, J. E. A. and Hasaneini, S. J. (2013). Neglected losses and key costs: tracking the energetics of walking and running. *J. Exp. Biol.* **216**, 933-938.
- Bertram, J. E. A. and Ruina, A. (2001). Multiple walking speed-frequency relations are predicted by constrained optimization. *J. Theor. Biol.* **209**, 445-453.
- Blickhan, R. and Full, R. (1993). Similarity in multilegged locomotion: bouncing like a monopode. *J. Comp. Physiol. A.* **173**, 509-517.
- Cavagna, G. A. (2006). The landing-take-off asymmetry in human running. *J. Exp. Biol.* **209**, 4051-4060.
- Doke, J. and Kuo, A. D. (2007). Energetic cost of producing cyclic muscle force, rather than work, to swing the human leg. *J. Exp. Biol.* **210**, 2390-2398.
- Doke, J., Donelan, J. M. and Kuo, A. D. (2005). Mechanics and energetics of swinging the human leg. *J. Exp. Biol.* **208**, 439-445.
- Donelan, J. M. and Kram, R. (2000). Exploring dynamic similarity in human running using simulated reduced gravity. *J. Exp. Biol.* **203**, 2405-2415.
- Farley, C. T. and Ferris, D. P. (1998). Biomechanics of walking and running: center of mass movements to muscle action. *Exerc. Sport Sci. Rev.* **26**, 253-286.
- Farley, C. T. and McMahon, T. A. (1992). Energetics of walking and running: Insights from simulated reduced-gravity experiments. *J. Appl. Physiol.* **73**, 2709-2712.
- Hasaneini, S. J., Macnab, C. J. B., Bertram, J. E. A. and Leung, H. (2013). The dynamic optimization approach to locomotion dynamics: human-like gaits from a minimally-constrained biped model. *Adv. Robot.* **27**, 845-859.
- Hasaneini, S. J., Schroeder, R. T., Bertram, J. E. A. and Ruina, A. (2017). The converse effects of speed and gravity on the energetics of walking and running. *bioRxiv*.
- He, J. P., Kram, R. and McMahon, T. A. (1991). Mechanics of running under simulated low gravity. *J. Appl. Physiol.* **71**, 863-870.
- Hedrick, T. L. (2008). Software techniques for two- and three-dimensional kinematic measurements of biological and biomimetic systems. *Bioinspir. Biomim.* **3**, 034001.
- Kram, R. and Taylor, C. R. (1990). Energetics of running: a new perspective. *Nature* **346**, 265-267.
- Kuo, A. D. (2001). A simple model of bipedal walking predicts the preferred speed-step length relationship. *J. Biomech. Eng.* **123**, 264.
- Long, L. L. and Srinivasan, M. (2013). Walking, running, and resting under time, distance, and average speed constraints: optimality of walk-run-rest mixtures. *J. R. Soc. Interface* **10**, 20120980.
- McMahon, T. A. and Cheng, G. C. (1990). The mechanics of running: how does stiffness couple with speed? *J. Biomech.* **23**, 65-78.
- Rashevsky, N. (1948). On the locomotion of mammals. *Bull. Math. Biophys.* **10**, 11-23.
- Ruina, A., Bertram, J. E. A. and Srinivasan, M. (2005). A collisional model of the energetic cost of support work qualitatively explains leg sequencing in walking and galloping, pseudo-elastic leg behavior in running and the walk-to-run transition. *J. Theor. Biol.* **237**, 170-192.
- Selinger, J. C., O'Connor, S. M., Wong, J. D. and Donelan, J. M. (2015). Humans can continuously optimize energetic cost during walking. *Curr. Biol.* **25**, 2452-2456.
- Slawinski, J., Billat, V., Koralsztein, J.-P. and Tavernier, M. (2004). Use of lumbar point for the estimation of potential and kinetic mechanical power in running. *J. Appl. Biomech.* **20**, 324-331.
- Srinivasan, M. and Ruina, A. (2006). Computer optimization of a minimal biped model discovers walking and running. *Nature* **439**, 72-75.
- Willems, P. A., Cavagna, G. A. and Heglund, N. C. (1995). External, internal and total work in human locomotion. *J. Exp. Biol.* **198**, 379-393.
- Winter, D. A. (2009). Anthropometry. In *Biomechanics and Motor Control of Human Movement*, 4th edn, pp. 82-106. Hoboken, NJ: John Wiley & Sons.



Movie 1. A representative subject displays the pronounced difference in center-of-mass running kinematics resulting from a change in gravity. In the first half of the video, the runner experiences normal gravity (9.8 m/s^2), and exhibits large vertical excursion of the center of mass during the flight phase. In the second half of the video, the runner experiences simulated lunar gravity (approximately one-sixth of Earth-normal), and the center-of-mass excursions in flight are comparatively shallow. In both cases, the treadmill speed is 2 m/s. The video is slowed by a factor of four. Consent to publish this video was obtained from the subject depicted.

Table S1. This file contains data used in the manuscript. Effective gravitational acceleration (g), mean vertical takeoff velocity (V), the standard error in the vertical takeoff velocity ($V \text{ Err}$), number of takeoffs measured during a trial ($N \text{ Takeoffs}$), mean ballistic height (H), standard error in ballistic height ($H \text{ Err}$), number of data points used for calculating mean ballistic height ($N \text{ H}$), and mean, standard error, and number of samples for stride frequency (f , $f \text{ Err}$, and $N \text{ f}$, respectively), are listed for all 50 trials. Leg length (l) is also reported for each subject. Data are grouped according to subject (ID code in first column) and, within each subject, listed in the order of measurement.

[Click here to Download Table S1](#)